International Journal of Scientific Research in Engineering and Management (IJSREM)
Volume: 03 Issue: 09 | Sept -2019 ISSN: 2590-1892

Control of DFIG Wind Power Generators in Unbalanced Microgrids Based on Instantaneous Power Theory

Arun Kumar. G

DEPARTMENT OF ELECTRICAL AND ELECTRONICS ENGINEERING & S R ENGINEERING COLLEGE

***Abstract*—This paper presents a model and a control strategy for a doubly-fed induction generator (DFIG) wind energy system in an unbalanced microgrid based on instantaneous power theory. The proposed model uses instantaneous real/reactive power components as the system state variables. In addition to the control of real/reactive powers, the controllers use the rotor-side converter for mitigating the torque and reactive power pulsations. The control scheme also uses the grid-side converter for partial compensation of unbalanced stator voltage. The main features of the proposed control method are its feedback variables are independent of reference frame transformations and it does not require sequential decomposition of current components. These features simplify the structure of required controllers under an unbalanced voltage condition and inherently improve the robustness of the controllers. A power limiting algorithm is also introduced to protect power converters against over rating and define the priority of real/reactive power references within the control scheme. The performance of the proposed strategy in reducing torque ripples and unbalanced stator voltage is investigated based on the time-domain simulation of a DFIG study system under unbalanced grid voltage.**

***Index Terms*—Doubly-fed induction generator, instantaneous power, microgrids, unbalanced grid voltage, wind energy.**

NOMENCLATURE

Symbol	*Definition*
$p,\ q,\ s$	real, reactive and complex power.
$\vec{\mathbf{v}},\ \vec{\mathbf{i}}$	voltage and current vectors.
$r,\ L,\ C$	resistance, inductance, and capacitance.
$P,\ J,\ T$	Pole pairs, inertia, and torque.
$\omega_e,\ \omega_{sl},\ \omega_r$	Synchronous, slip and rotor speeds.
$\theta_r,\ \theta_s$	Rotor angle and stator voltage vector angle.

Superscripts

$+\ ,\ -$	+/- sequence synchronous reference frame.
$\wedge\ ,\ *$	Complex conjugate and reference value.

Subscripts

$+\ ,\ -$	+/- sequence components.
$d,\ q$	Synchronous dq-axis.
$D,\ Q$	stationary DQ-axis.
$ave,\ ac,\ dc$	Average, pulsation, and dc components.
$s,\ r,\ g,\ l$	Stator, rotor, grid converter, and network.

I. INTRODUCTION

CURRENTLY, a huge amount of doubly-fed induction generators (DFIGs) in high-power wind turbine-generators (WTGs) are operational as distributed generators (DGs) units in microgrids. Recent grid codes require a WTG remains operational during transient and steady-state unbalanced grid voltages [1], [2]. A voltage unbalance can steadily exist in a microgrid due to unequal impedance of distribution lines; nonlinear loads such as arc furnaces; and unequal distributions of single-phase loads.

Shahnia *et al.* in [3] propose a distributed intelligent residential load transfer scheme to dynamically reduce voltage unbalance along low voltage distribution feeders. However, due to using widely distributed and variable loads such as single-phase motors, and nonlinear loads in a microgrid, the voltage unbalance condition cannot be completely mitigated. On the other hand, even a small amount of voltage unbalance can cause notable current unbalance in a DFIG. This current unbalance causes torque pulsations and overheating of the machine windings which eventually reduce the lifetime of a DFIG-based WTG in a microgrid [4]–[6].

Modeling and vector control of DFIG-based wind turbine under unbalanced conditions in microgrids are widely addressed in literature [7]–[11]. The existing unbalanced vector control schemes for DGs conventionally use two pairs of individual controllers for the positive and negative sequence components of unbalanced currents [12]–[15]. Tuning of these controllers due to the delays of the decomposing positive/negative sequences filters often requires complex algorithms in unbalanced vector control schemes [14], [15].

Alternative methods have been introduced which directly process the unbalanced rotor current without decomposition into positive/negative sequences [7], [8] and [16], [17]. However, in these methods, the calculation of current references based on the power pulsations also requires the positive and negative sequence components of the machine stator voltage, current, and flux. Direct power control (DPC)

methods have been also suggested for unbalanced voltage condition which relatively reduce the complexity of the control method compared to the vector control scheme [11], [18]–[20]. However, the DPC methods similar to the unbalanced vector control methods still need decomposition of positive/negative sequences and compensation for the filters delays.

This paper presents a control method for a DFIG connected to an unbalanced grid voltage, which uses the instantaneous real/reactive powers as the state variables. The proposed control approach offers a robust structure since its state variables are independent of the positive/negative sequences of the DFIG current components.

The suggested control scheme also reduces the DFIG torque/power pulsations by using the real/reactive power commands of the rotor-side converters in a DFIG wind energy system. Furthermore, at low wind speed and high unbalanced grid voltage conditions, the excess capacity of grid-side converter can be used for partial compensation of unbalanced stator voltage.

Two current/power limiting algorithms are also introduced for both rotor- and grid-side converters to avoid over rating of the converters. The performance of the proposed method under unbalanced grid voltage condition is investigated via time-domain simulation of a MW-scale DFIG wind turbine-generator study system in which a single-phase load is used to impose a steady voltage unbalance to the microgrid.

II. Conventional Vector Control Scheme for DFIG System Under Unbalanced Condition

Figure 1 shows the schematic diagram of a DFIG WTG including rotor-side (RSC) and grid-side (GSC) converters. Under balanced voltage condition, the converter controllers can be designed based on conventional vector control or other design techniques such as resonance controller and direct power control using instantaneous power model of the DFIG [17], [21]. However, under unbalanced voltage condition, auxiliary control loops using negative sequences quantities must be added to the conventional vector speed controllers which form an extended unbalanced vector control scheme [7], [17].

Figure 2 shows details of the unbalanced vector control scheme for the rotor-side converter [12], [13]. This control strategy mitigates the torque pulsations and the grid unbalanced effects on the generator via independent control of the stator real/reactive power components, p_s^* and q_s^*. The sequential decomposition unit in Fig. 2 calculates the positive/negative sequence components in postive/negative sequence qd reference frame. The output of this unit are denoted by $f_{+/-}^{+/-}$ where f represents the voltage or current quantities; superscripts identify +/- sequence reference frame; and subscripts represent +/- sequence components. In Fig. 2, the +/- reference frame transformations are realized by $e^{j(\theta_s-\theta_r)}$ and $e^{j(-\theta_s-\theta_r)}$.

As shown in Fig. 2, the unbalanced vector control method is established based on decompensation of the positive and negative sequences of the rotor current. Practically, this

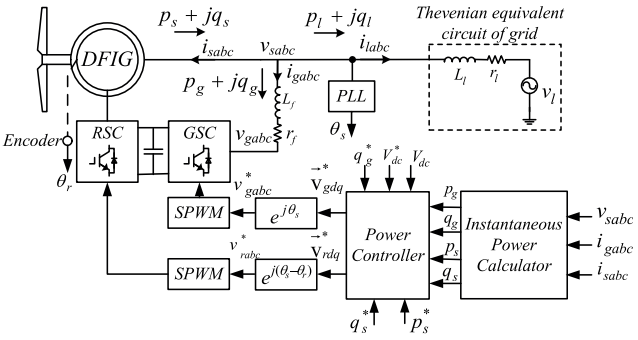

Fig. 1. Schematic diagram of DFIG-based Wind Generation System.

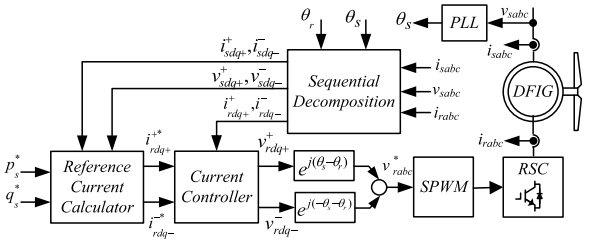

Fig. 2. Schematic diagram of the conventional unbalanced vector control scheme for DFIG [12], [13].

decomposition can be realized by transferring the current to the synchronous reference frame and using digital filters, or signal delay cancelation technique. These methods introduce time delays and obvious errors in amplitude and phase which adversely affect on the dynamic performance of the control system [20].

Recently, alternative methods such as the Proportional Integral Resonant (PIR) controller [7], [8] and the main and auxiliary controllers [16] have been introduced which directly process the unbalanced rotor current without decomposition into positive/negative sequences. In these methods, the current references are calculated according to the power pulsations in a feed-forward manner so the stator voltage, current, and flux have to be decomposed into the positive and negative sequences for calculating the rotor current references [20].

III. Proposed Instantaneous Power Control for Unbalanced Voltage Conditions

In the proposed method, the rotor-side converter in Fig. 1 can be used for the mitigation of the torque and stator reactive power pulsations. Also, the grid-side converter can be used for reduction of unbalanced stator voltage. In the proposed control method, the feedback loops are developed based on instantaneous real/reactive power components which can be directly calculated in *abc* frame and used in any other reference frame. In the following, first the instantaneous power model of a DFIG is explained and then the details of the proposed control strategy are explained within the following sections.

A. Instantaneous Power Model of a DFIG

The model of the induction machine in terms of the stator real/reactive power components, p_s and q_s, is [21]:

$$\frac{d}{dt}\begin{bmatrix} p_s \\ q_s \\ \psi_{sd} \\ \psi_{sq} \\ \omega_r \end{bmatrix} = \begin{bmatrix} g_1 & -\omega_{sl} & -g_4 & -g_5 & 0 \\ \omega_{sl} & g_1 & -g_5 & g_4 & 0 \\ \frac{2r_s v_{sd}}{3|v_s|^2} & \frac{2r_s v_{sq}}{3|v_s|^2} & 0 & \omega_e & 0 \\ \frac{2r_s v_{sq}}{3|v_s|^2} & -\frac{2r_s v_{sd}}{3|v_s|^2} & -\omega_e & 0 & 0 \\ g_6 & g_7 & 0 & 0 & 0 \end{bmatrix}\begin{bmatrix} p_s \\ q_s \\ \psi_{sd} \\ \psi_{sq} \\ \omega_r \end{bmatrix} + \begin{bmatrix} u_{rd} \\ u_{rq} \\ v_{sd} \\ v_{sq} \\ \frac{PT_m}{-J} \end{bmatrix} \tag{1}$$

where details of $u_{rd,rq}$ and g_1 to g_7 are given in Appendix.

The grid-side converter and filter model in terms of instantaneous real and reactive power of grid-side converter, p_g and q_g, is [22]:

$$\begin{bmatrix} \frac{dp_g}{dt} \\ \frac{dq_g}{dt} \end{bmatrix} = \begin{bmatrix} -\frac{r_f}{L_f} & -\omega_e \\ \omega_e & -\frac{r_f}{L_f} \end{bmatrix}\begin{bmatrix} p_g \\ q_g \end{bmatrix} + \frac{1}{L_f}\begin{bmatrix} u_{gd} \\ u_{gq} \end{bmatrix} \tag{2}$$

where

$$u_{gd} = \frac{3}{2}\Big(|v_s|^2 - \big(v_{gd}v_{sd} + v_{gq}v_{sq}\big)\Big), \tag{3}$$

and

$$u_{gd} = \frac{3}{2}\big(v_{gq}v_{sd} - v_{gd}v_{sq}\big). \tag{4}$$

The dynamic model of the dc link is:

$$\frac{dv_{dc}}{dt} = \frac{i_{dc}}{C} = \frac{p_g - p_r}{Cv_{dc}} \tag{5}$$

where the real power delivered to the rotor, p_r, is:

$$p_r = \frac{3}{2}\big(v_{rd}i_{rd} + v_{rq}i_{rq}\big). \tag{6}$$

Equations (1)-(6) summarize the model of a DFIG wind power system including the machine and converters.

B. Compensation of Unbalanced Voltage Using GSC

The excess capacity of grid-side converter at low wind speed can be used for a partial compensation of unbalanced stator voltage. This can be achieved through the control of the real/reactive power in GSC corresponding to the negative sequence of the grid voltage. This section develops the mathematical relationship between the power pulsation and the negative sequence voltage which is required in the design procedure of the control system.

The current/voltage vectors can be expressed in terms of their sequence components in +/- synchronous reference frames as:

$$\vec{\mathbf{f}}^{+}_{dq} = \vec{\mathbf{f}}^{+}_{dq+} + \vec{\mathbf{f}}^{+}_{dq-} = \vec{\mathbf{f}}^{+}_{dq+} + \vec{\mathbf{f}}^{-}_{dq-}e^{-j2\omega_e t} \tag{7}$$

Based on (7), the instantaneous real/reactive power components can be obtained via definition of complex power as:

$$\begin{aligned} s_g(t) = p_g(t) + jq_g(t) &= \frac{3}{2}\vec{\mathbf{v}}^{+}_{sdq}\hat{\vec{\mathbf{i}}}^{+}_{gdq} \\ &= \frac{3}{2}\Big(\vec{\mathbf{v}}^{+}_{sdq+} + \vec{\mathbf{v}}^{-}_{sdq-}e^{-j2\omega_e t}\Big)\Big(\hat{\vec{\mathbf{i}}}^{+}_{gdq+} + \hat{\vec{\mathbf{i}}}^{-}_{gdq-}e^{j2\omega_e t}\Big) \\ &= \frac{3}{2}\Big(\vec{\mathbf{v}}^{+}_{sdq+}\hat{\vec{\mathbf{i}}}^{+}_{gdq+} + \vec{\mathbf{v}}^{-}_{sdq-}\hat{\vec{\mathbf{i}}}^{-}_{gdq-}\Big) + \\ &+ \frac{3}{2}\Big(\vec{\mathbf{v}}^{+}_{sdq+}\hat{\vec{\mathbf{i}}}^{-}_{gdq-}e^{j2\omega_e t} + \vec{\mathbf{v}}^{-}_{sdq-}\hat{\vec{\mathbf{i}}}^{+}_{gdq+}e^{-j2\omega_e t}\Big), \end{aligned} \tag{8}$$

where $\hat{\vec{x}}$ represents the complex conjugate of $\vec{x}$. Substituting for $\hat{\vec{\mathbf{i}}}^{-}_{gdq-} = \hat{\vec{\mathbf{i}}}^{+}_{gdq-}e^{-j2\omega_e t}$ and $\vec{\mathbf{v}}^{-}_{sdq-} = \vec{\mathbf{v}}^{+}_{sdq-}e^{j2\omega_e t}$ in the last term of (8), we can express complex power in terms of its average and ac components as $s = s_{g,ave} + s_{g,ac}$ where:

$$s_{g,ave} = p_{g,ave} + jq_{g,ave} \triangleq \frac{3}{2}\Big(\vec{\mathbf{v}}^{+}_{sdq+}\hat{\vec{\mathbf{i}}}^{+}_{gdq+} + \vec{\mathbf{v}}^{-}_{sdq-}\hat{\vec{\mathbf{i}}}^{-}_{gdq-}\Big), \tag{9}$$

$$s_{g,ac} = p_{g,ac} + jq_{g,ac} \triangleq \frac{3}{2}\Big(\vec{\mathbf{v}}^{+}_{sdq+}\hat{\vec{\mathbf{i}}}^{+}_{gdq-} + \vec{\mathbf{v}}^{+}_{sdq-}\hat{\vec{\mathbf{i}}}^{+}_{gdq+}\Big). \tag{10}$$

Based on (10), control of power pulsations ($p_{g,ac}$ and $q_{g,ac}$) via grid-side converter can indirectly compensate unbalanced voltage by reducing $\vec{\mathbf{v}}^{+}_{sdq-}$.

To design power pulsation controllers, we start with the model of the grid-side converter and network in the positive synchronous reference frame as:

$$\vec{\mathbf{v}}^{+}_{sdq} - \vec{\mathbf{v}}^{+}_{gdq} = r_f\vec{\mathbf{i}}^{+}_{gdq} + L_f\frac{d\vec{\mathbf{i}}^{+}_{gdq}}{dt} + j\omega_e L_f\vec{\mathbf{i}}^{+}_{gdq}, \tag{11}$$

$$\vec{\mathbf{v}}^{+}_{sdq} - \vec{\mathbf{v}}^{+}_{ldq} = r_l\vec{\mathbf{i}}^{+}_{ldq} + L_l\frac{d\vec{\mathbf{i}}^{+}_{ldq}}{dt} + j\omega_e L_l\vec{\mathbf{i}}^{+}_{ldq}, \tag{12}$$

$$\vec{\mathbf{i}}^{+}_{gdq} = -\vec{\mathbf{i}}^{+}_{ldq} - \vec{\mathbf{i}}^{+}_{sdq}. \tag{13}$$

To obtain the power model for the negative sequence model, the negative sequence power components in the positive sequence reference frame are defined as:

$$s^{+}_{g-} \triangleq p^{+}_{g-} + jq^{+}_{g-} = \frac{3}{2}\vec{\mathbf{v}}^{+}_{sdq+}\hat{\vec{\mathbf{i}}}^{+}_{gdq-} \tag{14}$$

$$s^{+}_{s-} \triangleq p^{+}_{s-} + jq^{+}_{s-} = \frac{3}{2}\vec{\mathbf{v}}^{+}_{sdq+}\hat{\vec{\mathbf{i}}}^{+}_{sdq-} \tag{15}$$

By separating positive and negative sequences in (11)-(13) and using (14) and (15) to substitute for $\vec{\mathbf{i}}^{+}_{sdq-}$ and $\vec{\mathbf{i}}^{+}_{gdq-}$ in (11)-(13) and re-arranging the equation, we deduce:

$$\begin{aligned} \begin{bmatrix} \frac{dp^{+}_{g-}}{dt} \\ \frac{dq^{+}_{g-}}{dt} \end{bmatrix} &= \begin{bmatrix} -\frac{(r_f+r_l)}{(L_f+L_l)} & -\omega_e \\ \omega_e & -\frac{(r_f+r_l)}{(L_f+L_l)} \end{bmatrix}\begin{bmatrix} p^{+}_{g-} \\ q^{+}_{g-} \end{bmatrix} + \\ &+ \begin{bmatrix} \frac{r_l}{(L_f+L_l)} & \frac{\omega_e L_l}{(L_f+L_l)} \\ -\frac{\omega_e L_l}{(L_f+L_l)} & \frac{r_l}{(L_f+L_l)} \end{bmatrix}\begin{bmatrix} p^{+}_{s-} \\ q^{+}_{s-} \end{bmatrix} + \frac{L_l}{(L_f+L_l)}\begin{bmatrix} \frac{dp^{+}_{s-}}{dt} \\ \frac{dq^{+}_{s-}}{dt} \end{bmatrix} + \\ &+ \frac{1}{(L_f+L_l)}\begin{bmatrix} u^{+}_{ld-} - u^{+}_{gd-} \\ u^{+}_{lq-} - u^{+}_{gq-} \end{bmatrix} \end{aligned} \tag{16}$$

where the p^{+}_{s-}, q^{+}_{s-} are obtained from the negative sequence model of DFIG extracted from (1) in the positive sequence reference frame and

$$\begin{bmatrix} u^{+}_{ld-} \\ u^{+}_{lq-} \end{bmatrix} = \frac{3}{2}\begin{bmatrix} v^{+}_{sd+} & v^{+}_{sq+} \\ v^{+}_{sq+} & -v^{+}_{sd+} \end{bmatrix}\begin{bmatrix} v^{+}_{ld-} \\ v^{+}_{lq-} \end{bmatrix}, \tag{17}$$

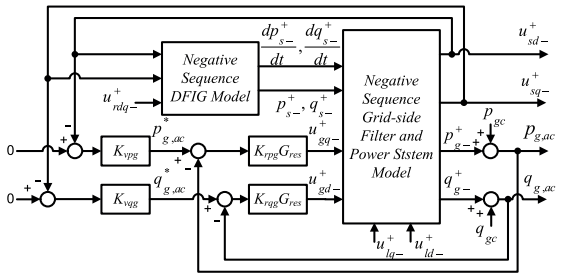

Fig. 3. Schematic diagram of the GSC model for compensating the negative sequence of the grid voltage.

$$\begin{bmatrix} u^+_{gd-} \\ u^+_{gq-} \end{bmatrix} = \frac{3}{2}\begin{bmatrix} v^+_{sd+} & v^+_{sq+} \\ v^+_{sq+} & -v^+_{sd+} \end{bmatrix}\begin{bmatrix} v^+_{gd-} \\ v^+_{gq-} \end{bmatrix}. \tag{18}$$

Let the output variables u^+_{sq-} and u^+_{sd-} are defined corresponding to the negative sequence of the stator voltage as:

$$\begin{bmatrix} u^+_{sd-} \\ u^+_{sq-} \end{bmatrix} = \frac{3}{2}\begin{bmatrix} v^+_{sd+} & v^+_{sq+} \\ v^+_{sq+} & -v^+_{sd+} \end{bmatrix}\begin{bmatrix} v^+_{sd-} \\ v^+_{sq-} \end{bmatrix} \tag{19}$$

Then, by substituting for $\vec{\mathbf{i}}^+_{gdq-}$ in terms of power components from (14) in (12), we deduce:

$$\begin{bmatrix} u^+_{sd-} \\ u^+_{sq-} \end{bmatrix} = \begin{bmatrix} u^+_{gd-} \\ u^+_{gq-} \end{bmatrix} + \begin{bmatrix} r_f/L_f & -\omega_e \\ \omega_e & r_f/L_f \end{bmatrix}\begin{bmatrix} p^+_{g-} \\ q^+_{g-} \end{bmatrix} + \begin{bmatrix} \frac{dp^+_{g-}}{dt} \\ \frac{dq^+_{g-}}{dt} \end{bmatrix} \tag{20}$$

Finally, to associate the negative sequence power components with the power pulsations, the new disturbance terms s_{gc}, p_{gc} and q_{gc} are defined as:

$$s_{gc} = p_{gc} + jq_{gc} \triangleq \vec{\mathbf{v}}^+_{sdq-}\hat{\vec{\mathbf{i}}}^+_{gdq+}. \tag{21}$$

Thus, based on (10), (14), and (21), we deduce:

$$p_{g,ac} = p^+_{g-} + p_{gc}, \quad q_{g,ac} = q^+_{g-} + q_{gc}. \tag{22}$$

Figure 3 shows the schematic diagram of the grid side converter model and DFIG in terms of power components based on (1) and (16)-(22). In this model, power pulsation references for GSC are used for adjusting the negative sequence grid voltage. Figure 4 depicts the proposed control system for grid-side converter. In this control system, G_{Pg}, G_{Qg} and G_{dc} controllers are designed based on balanced model as elaborated in [21]. Then, extra control loops including K_{vdg}, K_{vqg}, $K_{rpg}G_{res}$ and $K_{rqg}G_{res}$ are employed to control power pulsations of converter corresponding to pulsations of grid voltage at positive sequence reference frame. The resonant compensator (G_{res}) tuned at the double frequency of the grid which is implemented in the positive sequence reference frame. The notch filter G_{nf} is also used for suppressing the dc-link voltage double-frequency ($2\omega_e$) ripple. The transfer functions of resonant compensator and notch filter (G_{nf}) which are tuned at $\omega_0 = 2\omega_e$ frequency are:

$$G_{res} = \frac{\frac{\omega_0}{Q}s}{s^2 + \frac{\omega_0}{Q}s + \omega_0{}^2}, \quad G_{nf} = \frac{s^2 + \omega_0^2}{s^2 + \frac{\omega_0}{Q}s + \omega_0{}^2}, \tag{23}$$

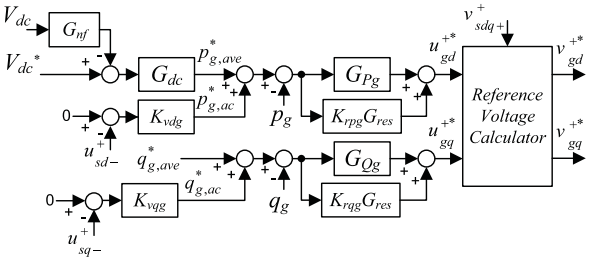

Fig. 4. Details of the proposed unbalanced controllers for the grid-side converter.

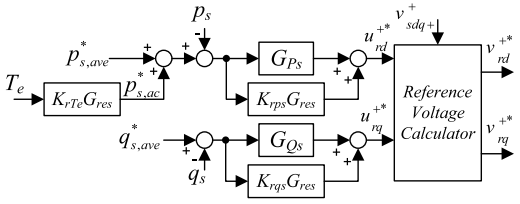

Fig. 5. Details of the proposed unbalanced controllers for the rotor-side converter.

where Q is the band-width of the filters. In the proposed control scheme, the instantaneous powers are controlled without decomposing the positive and negative sequences of currents. However, compensating of the unbalanced voltage requires the negative sequence of stator voltage at positive sequence reference frame.

C. Mitigation of Torque/Reactive Power Pulsations Using RSC

Although GSC to some extent can compensate the unbalanced grid voltage, the torque and power pulsations still exist due to $2\omega_e$ ripple which superimposed on the dc-link voltage. The torque pulsation in a generator increases stress on the rotating shaft of the DFIG which can cause shaft fatigue or other mechanical damages to a WTG. Thus, a control provision is required for the rotor-side converter to mitigate the torque/power pulsations of DFIG. Santos-Martin *et al.* in [23] show that the simultaneous elimination of the torque and real power pulsations can not be performed under unbalanced grid voltage condition. Thus, the proposed control scheme herein is designed to compensate the torque and reactive power pulsations as shown in Fig. 5. This control scheme essentially consists of two controllers, G_{Ps} and G_{Qs}, which are designed for a balanced condition as discussed [21]. Then, extra feedback control loops including $K_{rps}G_{res}$, $K_{rqs}G_{res}$ and $K_{rTe}G_{res}$ are added to compensate the double-frequency torque and reactive power pulsations without decomposing the positive and negative sequences of currents and voltages. The K_{rps}, K_{rqs} and K_{rTe} are constant gains and G_{res} is a band pass filter tuned at double frequency as given in (23). The electric torque can be estimated by stator and rotor current components in the stationary reference frame as

$$T_e = \frac{3PL_m}{2}\left(i_{sQ}i_{rD} - i_{sD}i_{rQ}\right). \tag{24}$$

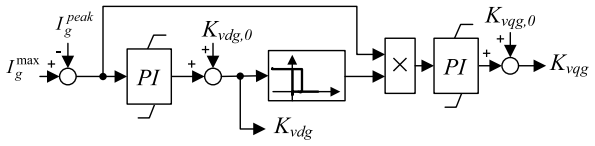

Fig. 6. The schematic of the power limiter for the grid-side converter.

The suggested control scheme in Fig. 5 can be alternatively used for elimination of real and reactive power pulsations if K_{rTe} is set to zero.

IV. Current/Power Limiting Algorithms for the Grid- and Rotor-Side Converters

Using power as a dynamic variable can cause over current of the power converter during transients and faults in a grid. This section presents an algorithm for limiting power references via sensing the converters currents.

A. Grid-Side Converter

In the control scheme for the grid-side converter (Fig. 4), the power capacity of the converter can be used for partially compensating the unbalanced stator voltage. However, it is necessary that the converter maintain the dc-link voltage via control of average real power and supplying the rotor real power has the highest priority. Thus, the maximum and minimum limits of average real power will be set to the maximum and minimum complex power as:

$$p_{g,ave}^{max} = -p_{g,ave}^{min} = S_g^{max} = \frac{3}{2}|v_s^+|I_g^{max}, \tag{25}$$

where S_g^{max} and I_g^{max} are the maximum complex power and maximum current of GSC, respectively. Then, the limits for average reactive power should be calculated with respect to instantaneous real power as given by:

$$q_{g,ave}^{max} = -q_{g,ave}^{min} = \sqrt{(S_g^{max})^2 - p_{g,ave}^2}, \tag{26}$$

The references for power pulsation components, Fig. 4, are:

$$p_{g,ac}^* = K_{vdg}u_{ds-}^+, \quad q_{g,ac}^* = K_{vqg}u_{qs-}^+. \tag{27}$$

Based on (27), Fig. 6 presents a method for limiting the power pulsation references via adjusting K_{vdg} and K_{vqg}. In this method K_{vdg} and K_{vqg} are initially set to pre-adjusted quantities K_{vdg0} and K_{vqg0}. The unbalanced grid voltage is compensated using these fixed gains until the peak current of converter (I_g^{peak}) passes its maximum limit. Then, in the first step, K_{vqg} is decreased to reduce the $q_{g,ac}^*$ and if $q_{g,ac}^*$ reaches zero and still I_g^{peak} is beyond its limit, then K_{vdg} is decreased to reduce $p_{g,ac}^*$. Therefore, the unbalanced grid voltage compensation can be partially or completely deactivated during the over current of the grid-side converter.

B. Rotor-Side Converter

Under a normal operating condition, the reference for the stator real power is adjusted to capture the maximum wind energy. This reference can be obtained via any maximum power point tracking (MPPT) algorithm [24]. The stator reactive power reference is also adjusted to satisfy the power factor requirements at the grid. Therefore, the maximum currents of the rotor and stator windings determine the upper limits of the generator real and reactive powers. Similar to the grid-side converter, the limits for the generator real/reactives can be obtained as:

$$p_s^{max1} = -p_s^{min1} = S_s^{max} = \frac{3}{2}|v_s^+|I_s^{max} \tag{28}$$

$$q_s^{max1} = -q_s^{min1} = \sqrt{(S_s^{max})^2 - p_s^2} \tag{29}$$

where I_s^{max} and S_s^{max} are the stator maximum current and complex power, respectively. Since the stator power is mainly controlled via the rotor-side converter (RSC), the limits of the rotor complex power should be adjusted based on the stator complex power. The rotor complex power is

$$s_r = p_r + jq_r = \frac{3}{2}\vec{\mathbf{v}}_{rdq}^+\hat{\vec{\mathbf{i}}}_{rdq}^+ \tag{30}$$

Assuming that the stator and rotor resistances in a high-power generator are small quantities, the rotor voltage/current can be approximately expressed by:

$$\vec{\mathbf{v}}_{rdq}^+ = \frac{L_m\omega_{sl}}{L_m\omega_e}\vec{\mathbf{v}}_{sdq}^+ + jL_r'\omega_{sl}\vec{\mathbf{i}}_{rdq}^+, \tag{31}$$

$$\vec{\mathbf{i}}_{rdq}^+ = -\frac{j\vec{\mathbf{v}}_{sdq}^+}{L_s\omega_e} - \frac{L_s}{L_m}\vec{\mathbf{i}}_{sdq}^+. \tag{32}$$

Substituting (31) and (32) in (30), we deduce:

$$\begin{aligned} s_r = p_r + jq_r &= \frac{3\omega_{sl}}{2\omega_e}\left(-\vec{\mathbf{v}}_{sdq}^+\hat{\vec{\mathbf{i}}}_{sdq}^+ + j\left(\frac{|v_s^+|^2}{L_s\omega_e} + L_r'\omega_e\left|\vec{\mathbf{i}}_{rdq}^+\right|\right)\right) \\ &= \frac{\omega_{sl}}{\omega_e}\left(p_s + j\left(q_s + \frac{3|v_s^+|^2}{2L_s\omega_e} + \frac{3}{2}L_r'\omega_e|i_r^+|\right)\right) \end{aligned} \tag{33}$$

Thus, the limits for the stator power components can be expressed as:

$$p_s^{max2} = -p_s^{min2} = \frac{\omega_e S_r^{max}}{\omega_{sl}} = \frac{3|v_s^+|I_r^{max}}{2N_{sr}}, \tag{34}$$

$$q_s^{max2} = -\frac{3|v_s^+|^2}{2L_s\omega_e} - \frac{3}{2}L_r'\omega_e|i_r^+|^2 + \sqrt{\left(\frac{3|v_s^+|I_r^{max}}{2N_{sr}}\right)^2 - p_s^2}, \tag{35}$$

$$q_s^{min2} = -\frac{3|v_s^+|^2}{2L_s\omega_e} - \frac{3}{2}L_r'\omega_e|i_r^+|^2 - \sqrt{\left(\frac{3|v_s^+|I_r^{max}}{2N_{sr}}\right)^2 - p_s^2}. \tag{36}$$

and the real/reactive power limits for the rotor-side converter can be defined as:

$$p_s^{min} = max\left(p_s^{min1}, p_s^{min2}\right), \quad p_s^{max} = min\left(p_s^{max1}, p_s^{max2}\right), \tag{37}$$

$$q_s^{min} = max\left(q_s^{min1}, q_s^{min2}\right), \quad q_s^{max} = min\left(q_s^{max1}, q_s^{max2}\right). \tag{38}$$

By using these limits during transients conditions, the capacity of RSC is partially used for injecting reactive power to the grid while the capacity of GSC is used for maintaining the dc-link voltage and compensation of unbalanced voltage.

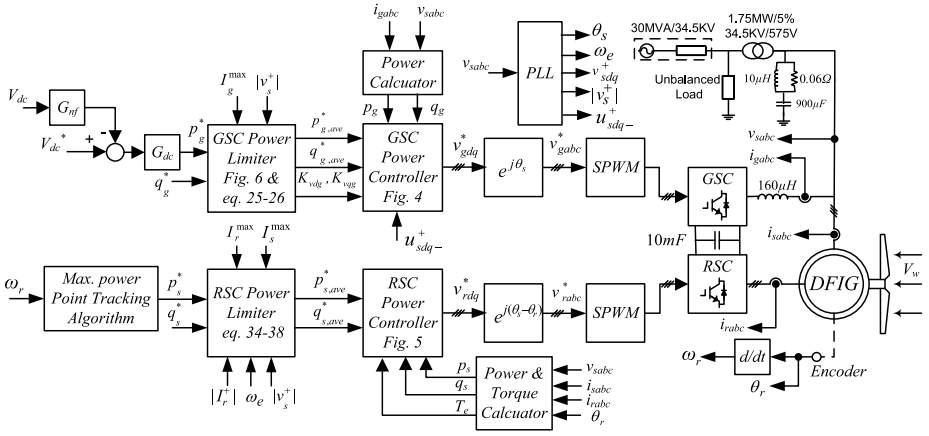

Fig. 7. Schematic diagram of the study system.

V. Performance Evaluation of the Power Control Scheme for Unbalanced Voltage Condition

A. Study System

Figure 7 shows the schematic of the study system for investigation of the performance and validation of the proposed control approach. The system includes a 1.5 MW DFIG wind turbine-generator connected to a weak grid including an unbalanced load. The electrical and mechanical parameters of the turbine generator are adopted from [25] and summarized in Table I. The control system of rotor-side converter presented in Fig. 5 is used for mitigation of the torque and stator reactive power pulsations via adjusting the stator real/reactive power. The stator real/reactive power references, p_s^* and q_s^*, are adjusted to capture the maximum wind energy and to meet a desired power factor, respectively. The real power reference, p_s^*, can be determined with respect to a feedback from the shaft rotor speed, ω_r, based on any Maximum Power Point Tracking (MPPT) algorithm [24]. The controller of grid-side converter presented in Fig. 4 is used to control real and reactive power and to mitigate unbalanced stator voltage. The parameters for balance operating condition are designed based on detailed method described in [21] as:

$$G_{P_s} = 1.33\left(1+\frac{10}{s}+\frac{s}{166.25}\right)\left(\frac{1}{1+0.016s}\right),$$
$$G_{Q_s} = 2.65\left(1+\frac{10}{s}+\frac{s}{331.25}\right)\left(\frac{1}{1+0.0032s}\right),$$
$$G_{P_g} = G_{Q_g} = \frac{2.65s+26.5}{s}, \quad G_{dc} = \frac{4.35s+8.7}{s},$$
$$G_{res} = \frac{7.54s}{s^2+7.54s+568489}, \quad G_{nf} = \frac{s^2+568489}{s^2+7.54s+568489}.$$

and the rest of constant parameters in controllers are:

$$K_{rTe} = 10, \quad K_{vdg} = K_{vqg} = 20, \; K_{rps} = 132.5,$$
$$K_{rqs} = 26.5, \; K_{rpg} = 2.65, \quad K_{rqg} = 2.65.$$

An 800 kW single phase inductive load with 0.8 power factor is connected to the phase a at the point of common coupling as shown on Fig. 7 which creates a 0.03 pu negative sequence voltage at generator stator.

TABLE I
Study System Parameters and Data

Parameters	Values	Units
Rated Power	1.5	[Mw]
Rated Voltage (Line-to-Line)	0.575	[kV]
Rated Frequency	60	[Hz]
Rated Wind Speed	12.0	[m/s]
Stator resistance	1.4	[mΩ]
Rotor resistance	0.99	[mΩ]
Stator leakage inductance	89.98	[μH]
Rotor leakage inductance	82.08	[μH]
Magnetization inductance	1.526	[mH]
Stator/rotor turns ratio	0.38	-
Poles	6	-
Turbine rotor diameter	70	[m]
Lumped inertia constant	5.04	[s]

B. Performance Evaluation of the Controllers

Figures 8, 9 and 10 compare the performance of the DFIG using balanced control, unbalanced vector control and proposed unbalanced control strategies under unbalanced voltage condition. The wind speed is $V_w = 11m/s$ corresponding to $p_s = 0.7$pu. The reference of reactive power is initially -0.8 pu increasing in two steps up to -0.35 and +0.15 pu to investigate the tracking performance of the controllers. Figure 8 shows the performance of the designed controllers for balanced condition in Fig. 1, when they are used under unbalanced condition. As Fig. 8(b) shows, the reactive power follows the two-step commands at $t = 0.1$ s and $t = 0.3$ s, however, double frequency pulsations appear in both powers and torque quantities [Fig. 8(a)-(c)] due to the unbalanced load condition. The amplitudes of the real/reactive power and torque pulsations are 0.1, 0.13 and 0.12 pu, respectively. Also, Fig. 8(d) shows that both stator and rotor currents include double-frequency ripples.

Figure 9 shows the performance of the unbalanced vector controller [Fig. 2] under unbalanced condition. As Fig. 9 shows the vector controllers significantly mitigate the power/torque pulsations. However, the sequential decomposition involved in the unbalanced vector controller will slow down the dynamic response of the current control loop and

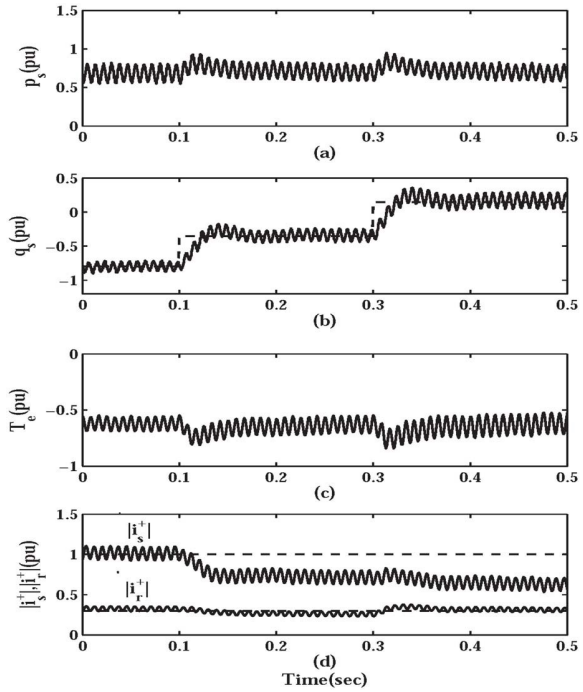

Fig. 8. The DFIG performance under unbalanced voltage using balanced controller: (a) stator real power; (b) stator reactive power; (c) torque; (d) stator and rotor currents.

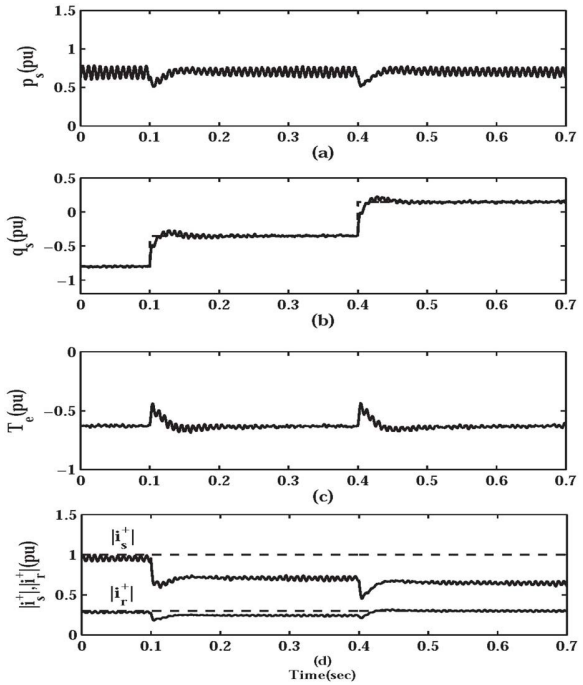

Fig. 9. Unbalanced vector controller: (a) stator real power; (b) stator reactive power; (c) torque; (d) stator and rotor currents.

consequently results in torque and power pulsations during transient conditions.

Figure 10 shows the performance of controllers under unbalanced condition when the proposed unbalanced controllers are used for the rotor- and grid-side converters. As Fig. 10 shows the proposed controllers significantly mitigate

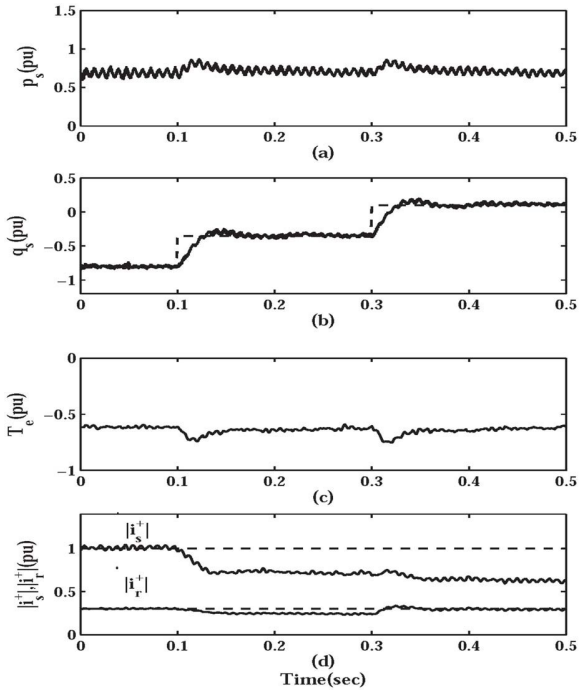

Fig. 10. The proposed controller: (a) stator real power; (b) stator reactive power; (c) torque; (d) stator and rotor currents.

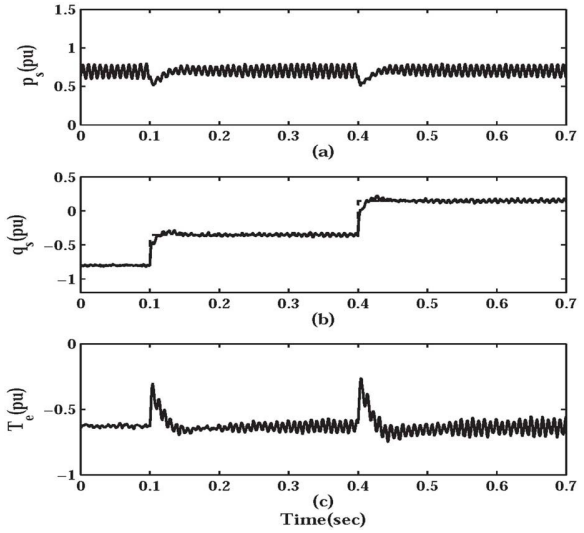

Fig. 11. Robustness of the unbalanced vector controller: (a) stator real power; (b) stator reactive power; (c) torque.

the power/torque pulsations compared with the conventional controllers [Fig. 8].

Comparing the torques in Figs. 9(c) and 10(c) shows that the proposed controller can control the torque with less double frequency ripples particularly at transients in $t = 0.1$ and 0.3 s. The reason is that the proposed controller uses the instantaneous real/reactive powers that are directly obtained from the *abc* reference frame voltage and current. However, in vector control method, the state variables are obtained from sequential decomposition in *qd* reference frame which in turn impacts on the performance of the vector control feedback control loops.

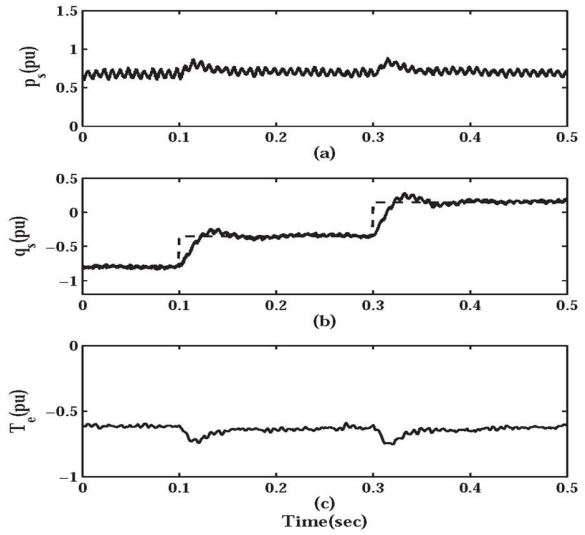

Fig. 12. Robustness of the proposed controller: (a) stator real power; (b) stator reactive power; (c) torque.

C. Robustness of the Controllers

To investigate the robustness of the proposed control method, the machine inductance (L_l) is changed and the performance of the vector controller is compared against the proposed control method. Figures 11 and 12 compare the robustness of unbalanced vector control and the proposed control strategies, respectively, in which L_l is reduced to 80% of its nominal value.

As Figs. 11(c) and 12(c) show, the unbalanced vector controller is more sensitive than the proposed controller to compensate the torque pulsation. The reason is that the unbalanced vector control method is more sensitive to the machine parameters that are used for the calculation of reference currents in its feedback control loops.

D. Partial Compensation of the Unbalanced Voltage

Figure 13 describes a scenario in which the grid-side converter can partially compensate the voltage unbalance. In this scenario, the wind speed is assumed $V_w = 12\ m/s$ to generate the rated power. Initially, the system operates under balance condition and the unbalanced load is connected at $t = 0.5\ s$. Thus, the negative sequence of the stator voltage increases up to 0.038 pu at $t = 0.5\ s$ as shown in Fig. 13(a). At $t = 1\ s$ the GSC is forced to reduce its real power from 0.8 pu to 0.45 pu [Fig. 13(b)] to leave the capacity of the GSC for partial compensation of unbalanced voltage. The compensation is performed via injection of negative sequence current to the grid [Fig. 13(d)] which decreases the negative sequence of the voltage down to 0.02 pu [Fig. 13(a)].

In this compensation scenario, the negative sequence current component of the GSC increases up to 0.22 pu [Fig. 13(d)] and due to the activation of the limiters the electric torque and the positive sequence current decrease to -0.4 pu and 0.08 pu, as shown in Figs. 13(c) and (e), respectively. This causes the amplitude of the GSC current (sum of the positive and negative current sequences) to be limited at its pre-specific level, i.e., 0.3 pu, as shown in Fig. 13(f).

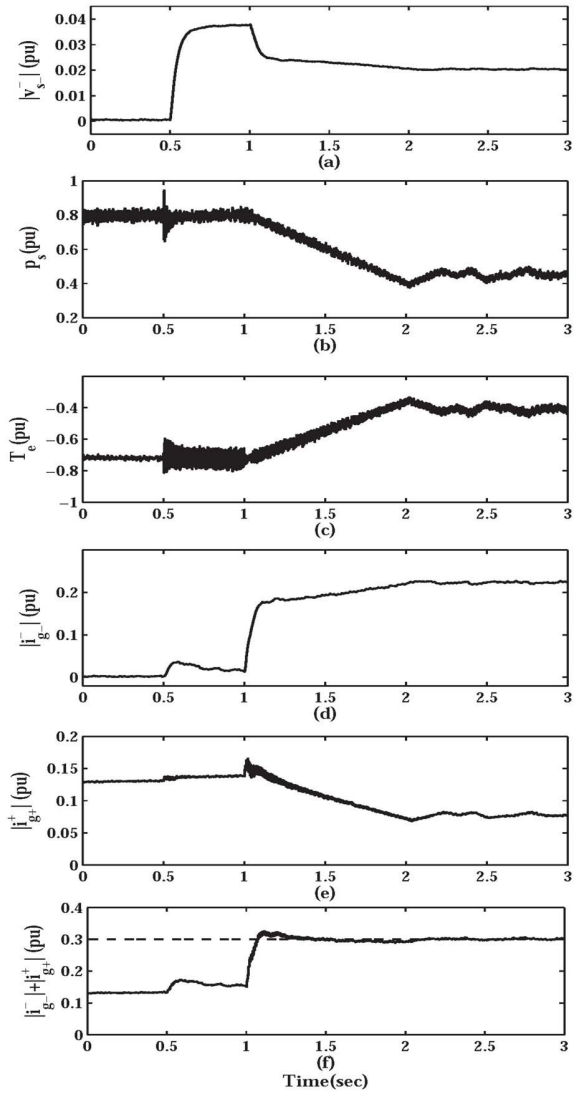

Fig. 13. Partial compensation of unbalanced stator voltage: (a) negative sequence of the stator voltage; (b) stator real power; (c) torque; and (d) negative sequence grid-side converter current. (e) positive sequence grid-side converter current; (f) amplitude of the grid-side converter current.

VI. Conclusion

An unbalanced control scheme for a DFIG wind turbine-generator has been presented in this paper which does not require the sequential decomposition of the DFIG stator/rotor currents and is less sensitive to the system parameters. This control scheme mitigates the stator reactive power and torque pulsations which obviously appears in any balanced control scheme under an unbalanced grid voltage condition. The control method uses the grid-side converter to partially compensate the unbalance stator voltage when the wind speed is low and turbine works below nominal power. Two current/power limiting algorithms are also introduced for both rotor- and grid-side converters to avoid over rating of the converters. It has been shown that proposed control approach based on its simple and robust structure can offer a promising solution for DFIG control under unbalanced grid voltage conditions.

APPENDIX

$$u_{rd} = g_2 v_{rd} + g_3 v_{rq} - \frac{3|v_s|^2}{2L'_s}, \quad u_{rq} = g_3 v_{rd} - g_2 v_{rq}, \tag{39}$$

$$g_1 = -\frac{r_s L_r + L_s r_s}{L'_s L_r}, \quad g_2 = \frac{3L_m v_{sd}}{2L_r L'_s}, \quad g_3 = \frac{3L_m v_{sq}}{2L_r L'_s},$$
$$g_4 = \frac{3}{2}\left(\frac{r_r v_{sd} - L_r \omega_r v_{sq}}{L'_s L_r}\right), \quad g_5 = \frac{3}{2}\left(\frac{r_r v_{sq} + L_r \omega_r v_{sd}}{L'_s L_r}\right).$$
$$g_6 = \frac{P^2}{J}\frac{\psi_{sq} v_{sd} - \psi_{sd} v_{sq}}{|v_s|^2}, \quad g_7 = \frac{P^2}{J}\frac{\psi_{sd} v_{sd} + \psi_{sq} v_{sq}}{|v_s|^2}. \tag{40}$$

REFERENCES

[1] M. Mohseni and S. M. Islam, "Review of international grid codes for wind power integration: Diversity, technology and a case for global standard," *Renew. Sustain. Energy Rev.*, vol. 16, no. 6, pp. 3876–3890, 2012.

[2] C. Jauch, J. Matevosyan, T. Ackermann, and S. Bolik, "International comparison of requirements for connection of wind turbines to power systems," *Wind Energy*, vol. 8, no. 3, pp. 295–306, 2005.

[3] F. Shahnia, P. J. Wolfs, and A. Ghosh, "Voltage unbalance reduction in low voltage feeders by dynamic switching of residential customers among three phases," *IEEE Trans. Smart Grid*, vol. 5, no. 3, pp. 1318–1327, May 2014.

[4] R. Piwko *et al.*, "Integrating large wind farms into weak power grids with long transmission lines," in *Proc. CES/IEEE 5th Int. Power Electron. Motion Control Conf. (IPEMC)*, vol. 2. Dalian, China, 2006, pp. 1–7.

[5] K. Lee, T. M. Jahns, W. E. Berkopec, and T. A. Lipo, "Closed-form analysis of adjustable-speed drive performance under input-voltage unbalance and sag conditions," *IEEE Trans. Ind. Appl.*, vol. 42, no. 3, pp. 733–741, May/Jun. 2006.

[6] E. Nasr-Azadani, C. A. Cañizares, D. E. Olivares, and K. Bhattacharya, "Stability analysis of unbalanced distribution systems with synchronous machine and DFIG based distributed generators," *IEEE Trans. Smart Grid*, vol. 5, no. 5, pp. 2326–2338, Sep. 2014.

[7] H. Xu, J. Hu, and Y. He, "Integrated modeling and enhanced control of DFIG under unbalanced and distorted grid voltage conditions," *IEEE Trans. Energy Convers.*, vol. 27, no. 3, pp. 725–736, Sep. 2012.

[8] J. Hu and Y. He, "DFIG wind generation systems operating with limited converter rating considered under unbalanced network conditions—Analysis and control design," *Renew. Energy*, vol. 36, no. 2, pp. 829–847, 2011.

[9] Y. Yan, M. Wang, Z.-F. Song, and C.-L. Xia, "Proportional-resonant control of doubly-fed induction generator wind turbines for low-voltage ride-through enhancement," *Energies*, vol. 5, no. 11, pp. 4758–4778, 2012.

[10] C. Liu, F. Blaabjerg, W. Chen, and D. Xu, "Stator current harmonic control with resonant controller for doubly fed induction generator," *IEEE Trans. Power Electron.*, vol. 27, no. 7, pp. 3207–3220, Jul. 2012.

[11] P. Zhou, Y. He, and D. Sun, "Improved direct power control of a DFIG-based wind turbine during network unbalance," *IEEE Trans. Power Electron.*, vol. 24, no. 11, pp. 2465–2474, Nov. 2009.

[12] Y. Zhou, P. Bauer, J. A. Ferreira, and J. Pierik, "Operation of grid-connected DFIG under unbalanced grid voltage condition," *IEEE Trans. Energy Convers.*, vol. 24, no. 1, pp. 240–246, Mar. 2009.

[13] L. Xu and Y. Wang, "Dynamic modeling and control of DFIG-based wind turbines under unbalanced network conditions," *IEEE Trans. Power Syst.*, vol. 22, no. 1, pp. 314–323, Feb. 2007.

[14] M. Savaghebi, A. Jalilian, J. C. Vasquez, and J. M. Guerrero, "Secondary control scheme for voltage unbalance compensation in an islanded droop-controlled microgrid," *IEEE Trans. Smart Grid*, vol. 3, no. 2, pp. 797–806, Jun. 2012.

[15] M. Hamzeh, H. Karimi, and H. Mokhtari, "Harmonic and negative-sequence current control in an islanded multi-bus MV microgrid," *IEEE Trans. Smart Grid*, vol. 5, no. 1, pp. 167–176, Jan. 2014.

[16] L. Xu, "Enhanced control and operation of DFIG-based wind farms during network unbalance," *IEEE Trans. Energy Convers.*, vol. 23, no. 4, pp. 1073–1081, Dec. 2008.

[17] V.-T. Phan and H.-H. Lee, "Performance enhancement of stand-alone DFIG systems with control of rotor and load side converters using resonant controllers," *IEEE Trans. Ind. Appl.*, vol. 48, no. 1, pp. 199–210, Jan./Feb. 2012.

[18] G. Abad, M. A. Rodriguez, G. Iwanski, and J. Poza, "Direct power control of doubly-fed-induction-generator-based wind turbines under unbalanced grid voltage," *IEEE Trans. Power Electron.*, vol. 25, no. 2, pp. 442–452, Feb. 2010.

[19] J. Alonso-Martinez, J. Eloy-Garcia, D. Santos-Martin, and S. Arnaltes, "A new variable-frequency optimal direct power control algorithm," *IEEE Trans. Ind. Electron.*, vol. 60, no. 4, pp. 1442–1451, Apr. 2013.

[20] H. Nian, Y. Song, P. Zhou, and Y. He, "Improved direct power control of a wind turbine driven doubly fed induction generator during transient grid voltage unbalance," *IEEE Trans. Energy Convers.*, vol. 26, no. 3, pp. 976–986, Sep. 2011.

[21] E. Rezaei, A. Tabesh, and M. Ebrahimi, "Dynamic model and control of DFIG wind energy systems based on power transfer matrix," *IEEE Trans. Power Del.*, vol. 27, no. 3, pp. 1485–1493, Jul. 2012.

[22] A. Tabesh and R. Iravani, "Multivariable dynamic model and robust control of a voltage-source converter for power system applications," *IEEE Trans. Power Del.*, vol. 24, no. 1, pp. 462–471, Jan. 2009.

[23] D. Santos-Martin, J. L. Rodriguez-Amenedo, and S. Arnalte, "Direct power control applied to doubly fed induction generator under unbalanced grid voltage conditions," *IEEE Trans. Power Electron.*, vol. 23, no. 5, pp. 2328–2336, Sep. 2008.

[24] M. R. Patel, *Wind and Solar Power Systems: Design, Analysis, and Operation*. Boca Raton, FL, USA: CRC Press, 2006.

[25] R. Fadaeinedjad, M. Moallem, and G. Moschopoulos, "Simulation of a wind turbine with doubly fed induction generator by FAST and Simulink," *IEEE Trans. Energy Convers.*, vol. 23, no. 2, pp. 690–700, Jun. 2008.